Science Journal of Chemistry
2020; 8(2): 28-35
http://www.sciencepublishinggroup.com/j/sjc
doi: 10.11648/j.sjc.20200802.12
ISSN: 2330-0981 (Print); ISSN: 2330-099X (Online)

Review Article

Review on In-depth Analysis of the Passive Films of W-xTi Alloys by Angle Resolved X-Ray Photoelectron Spectroscopy

Jagadeesh Bhattarai

Central Department of Chemistry, Tribhuvan University, Kirtipur, Kathmandu, Nepal

Email address:
bhattarai_05@yahoo.com

To cite this article:
Jagadeesh Bhattarai. Review on In-depth Analysis of the Passive Films of W-xTi Alloys by Angle Resolved X-Ray Photoelectron Spectroscopy. *Science Journal of Chemistry*. Vol. 8, No. 2, 2020, pp. 28-35. doi: 10.11648/j.sjc.20200802.12

Received: February 29, 2020; **Accepted**: March 16, 2020; **Published**: April 28, 2020

Abstract: Spontaneously passivated sputter-deposited W-22Ti and W-58Ti alloys showed higher corrosion resistance than those of tungsten and titanium metals in 12 M HCl solution open to air at 30°C. Average corrosion rates of W-(22-58)Ti alloys (that is, about 9.5-18.5 × 10^{-3} mm/y) were found to be about three and half orders of magnitude lower than titanium and even lower than that of tungsten metal. Such synergistic effect of the simultaneous additions of tungsten and titanium in the extremely high corrosion resistance properties of the sputter-deposited amorphous/nanocrystalline W-xTi alloys was investigated using angle resolved X-ray photoelectron spectroscopic (ARXPS) analyses. In-depth surface analyses of the thin passive films of the W-xTi alloys using angle resolved XPS analyses revealed that the high corrosion resistance of the amorphous/nanocrystalline W-xTi alloys is mostly due to the formation of homogeneous passive double oxyhydroxide films consisting of W^{ox} and Ti^{4+} cations without any concentration gradient in-depth in 12 M HCl solution at 30°C. Consequently, titanium metal acts synergistically with tungsten in enhancing the spontaneous passivity as well as the high corrosion resistance of the sputter-deposited binary W-xTi alloys.

Keywords: Depth-profiling, Corrosion-resistant, Sputter Deposit, Binary Alloys, Aggressive Environment, XPS

1. Introduction

The non-destructive angle resolved XPS (ARXPS) technique is widely used by number of researchers to gain the in-depth concentration profiles of thin films for last five decades [1-7] after a valuable contribution of Kai Siegbahn and his research groups [8], because it proves as one of the promising in-depth surface analyses of the films to investigate chemical compositions, oxidation states, chemical shifts, binding energies and electronic structures of the films. In principle, the in-depth information of the passive films depends on the effective escape depth of the ejected photoelectrons, which increases with an increase in take-off angle of photoelectrons relative to the sample surface [1-7, 9-11]. Therefore, the surface sensitivity is varied by changing the take-off angle of photoelectrons (θ) as depicted in Figure 1.

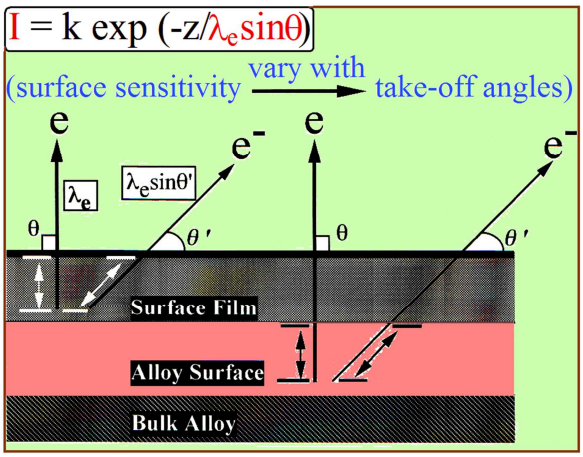

Figure 1. *A schematic diagram of the three layer model for the in-depth surface analyses of the sputter-deposited W-xTi alloys.*

At a lower value of θ, the intensity signals (I) from the surface of sample species located in the exterior part of the surface films are enhanced. Therefore, the apparent composition of the surface films formed on the binary alloys like sputter-deposited W-xTi alloys is changed with θ in the ARXPS measurements. Such in-depth profiling technique was reported to be effective to examine the formation of homogeneous or heterogeneous passive surface films formed on different types of sputter deposited corrosion-resistant alloys [12-22].

Tungsten is corrosion-resistant in non-oxidizing environments and titanium is widely recognized as corrosion-resistant metal in oxidizing environments. On the other hand, both tungsten and titanium are regarded as effective alloying elements for enhancing the corrosion resistance properties of the sputter-deposited alloys in aggressive environments. It is meaningful to mention here that the sputter-deposited alloys consisting of either amorphous or nanocrystalline phases were found chemically homogeneous [23] and hence the sputter-deposited tungsten-based binary and ternary alloys showed higher corrosion resistance than those of alloy-constituting elements in aggressive electrolytes [15-18, 20-22, 24–45]. The alloying of titanium with nickel [46, 47], chromium [14, 48], molybdenum [13, 49], tungsten [50–54] and manganese [55] greatly improved the corrosion resistance properties of the binary sputter-deposited alloys in aggressive environments and these alloys were passivated spontaneously in aggressive chloride containing environments. The significant improvement of the corrosion resistance behavior of these sputter-deposited binary and ternary alloys was attributed to the formation of homogeneous double oxyhydroxide passive films from the surface sensitive XPS analyses. Furthermore, in recent years, the Ti-M (M = W, Mo) alloys are considered as promising materials for fusion devices [56-59], high strength structural materials [58] and metallic biomaterials [60, 61], owing to their excellent mechanical properties, good biocompatibility with high chemical stability in the physiological environments. In this context, the present research work was aimed to clarify the mechanism of the higher corrosion resistance of the sputter-deposited W-22Ti and W-58Ti alloys than those of tungsten and titanium in 12 M HCl solution open to air at 30°C using angel resolved XPS technique.

2. Materials and Experiments

The sputter-deposited nanocrystalline W-22Ti and amorphous W-58Ti alloys having the apparent grain size of about 19 and 1.5 nm [53], respectively, were used to discuss the present work. Scherrer's equation [41, 62] was used to estimate the grain size of the alloys. The details about the preparation and characterization of these alloys were reported elsewhere [53]. The alloys' composition is expressed in atomic percentage (at %) hereinafter. The sputter-deposited W-xTi alloy specimens were mechanically polished with a silicon carbide paper up to grit number 1500 in cyclohexane, degreased by acetone and dried in air before the corrosion tests and angle resolved XPS analyses. The average corrosion rate of the alloys was estimated using weight loss method [63, 64] after immersion for 168 h in 12 M HCl solution open to air at 30°C.

The composition of the thin films formed on the W-xTi alloys was analyzed by angle-resolved XPS technique. Before and after immersion in 12 M HCl solution, XPS spectra were measured by a Shimadzu ESCA–850 photoelectron spectrometer with Mg K_α (hν = 1253.6 eV) radiation for surface analyses including the in-depth distribution of the species present in the surface of the alloys. XPS spectra for both the nanocrystalline W-22Ti and amorphous W-58Ti alloys exhibited peaks of tungsten, titanium, carbon, oxygen and chlorine over a wide binding energy region (that is, 0-1000 eV). The most intense peaks of the W 4f, Ti 2p, O 1s, Cl 2p and C 1s electrons were measured in the binding energy range of 20 eV for all spectra. The C 1s peak at range of 285.0 eV was used to calibrate the surface charging effect. For the alloy specimens after immersed in 12 M HCl solution, a very weak Cl 2p spectrum was detected at about 199.0 eV. However, the concentration of the chloride ion was not considered for the quantitative analyses of the surface films in this study because the intensity of the chloride ion is very low. The O 1s spectrum was composed of two peaks; the lower binding energy peak at 530.4 eV was assigned to OM oxygen, and the higher binding energy peak at 532.3 eV was assigned to OH oxygen [65].

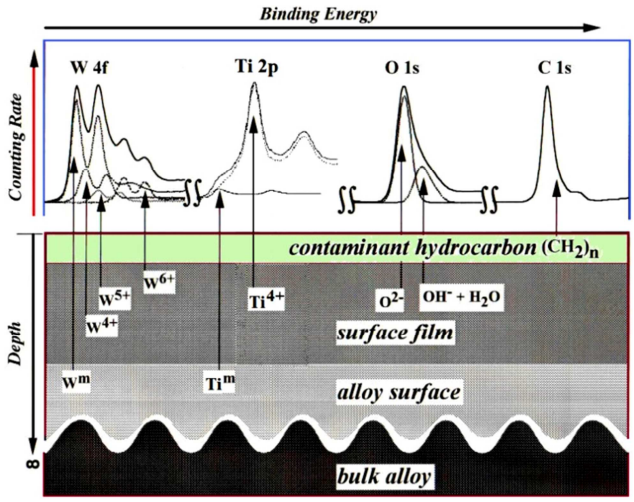

Figure 2. *A diagrammatic sketch of the three layers model for the quantitative XPS analyses of the surface films formed on the sputter-deposited W-xTi alloys.*

The spectra from the W-xTi alloys constituents indicated the presence of the oxidized and metallic species; the former comes from the surface film and the latter from the underlying alloy surface. The measured spectrum of W 4f electron was separated into W^{ox} 4f and W^0 4f and the measured spectrum of Ti 2p electron was separated into Ti^{4+} 2p and Ti^0 2p for the sputter-deposited W-xTi alloys. Furthermore, the W^0 4f spectrum was consisted of W^{4+}4f, W^{5+} 4f and W^{6+} 4f spectra. The integrated intensities of the W^0 4f, W^{4+} 4f, W^{5+} 4f, W^{6+} 4f, Ti^0 2p, and Ti^{4+} 2p were obtained by the same method as those described elsewhere [53, 65, 66]. The photo-ionization cross-section of the W 4f and Ti 2p electrons relative to the O 1s electrons used were 2.97 [67] and 1.2775 [46], respectively,

for quantitative analysis. After the integrated intensities of these all spectra observed from the surfaces of the sputter-deposited W-xTi alloys were obtained, the compositions and thickness of the passive films and the compositions of the underlying alloy surfaces were quantitatively determined using three layers model proposed by Asami *et al.* [65, 66]. The diagrammatic sketch of the three layers model for the W-xTi alloys is shown in Figure 2.

For angle-resolved XPS, the angle between the alloy specimen surface and the direction of photoelectron to the detector (take-off angle of photoelectrons) was changed by using tilted-specimen holders at 30°, 45°, 60° and 90°.

3. Results and Discussion

The corrosion rates of the sputter-deposited W-xTi alloys and alloy-constituting elements (that is, tungsten and titanium) were estimated from weight losses after immersion for 168 h in 12 M HCl solution open to air at 30°C considering uniform corrosion over the entire alloy surface with respect to immersion time. In order to obtain precise data and reproducibility, the corrosion rate of each specimen was estimated in triplicate and the average value was considered. Figure 3 shows the average corrosion rates of the tungsten and titanium metals which were found to be 2.76×10^{-2} mm/y and 5.9×10^{1} mm/y, respectively, in 12 M HCl solution. By contrast, the W-22Ti and W-58Ti alloys showed even lower corrosion rates (that is, about 1.0×10^{-2} mm/y or low) than those of alloy-constituting elements, i.e., tungsten and titanium metals. Consequently, it can be said that both tungsten and titanium metals improve the corrosion resistance properties of the sputter–deposited W-22Ti and W-58Ti alloys synergistically.

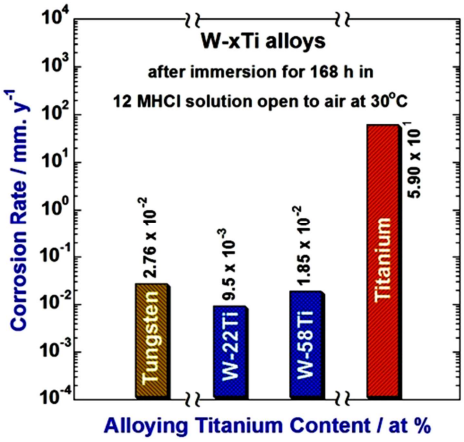

Figure 3. *Corrosion rates of the sputter-deposited W-xTi alloys including the sputter-deposited tungsten and titanium after immersion for 168 h in 12 M HCl solution open to air at 30 °C.*

The similar effect was previously reported for other sputter-deposited W-xTi alloys in HCl solutions [52, 53], mostly due to the synergistic effect of tungsten and titanium in forming the double oxyhydroxide which was responsible for the higher corrosion resistance of the sputter-deposited W-xTi alloys than those of the alloy-constituting elements in HCl solutions from the conventional XPS analyses [53]. The experimental results of the ARXPS measurements are presented here to clarify the mechanism of showing such higher corrosion resistance behavior of the sputter-deposited binary W-xTi alloys than those of alloy-constituting elements in 12 M HCl solution. In general, the in-depth surface analysis using ARXPS technique is carried out for a better understanding of the effects of alloy-constituting elements in the corrosion-resistant behavior of the sputter-deposited binary alloys to know whether the passive films formed on the alloys are homogeneous or not [12, 17, 20, 22].

The spectra from the W-xTi alloys indicated the presence of the oxidized and metallic species; the former comes from the surface film and the latter from the underlying alloy surface [53]. The measured spectrum of Ti 2p electron was separated into Ti^{4+} 2p and Ti^{0} 2p spectra as shown in Figure 4 (a) and the measured spectrum of W 4f electron was separated into W^{0} 4f and W^{ox} 4f spectra as shown in Figure 4 (b) for the sputter-deposited W-58Ti alloy. The Ti^{4+} 2p and Ti^{0} 2p spectra were consisted of lower and higher binding energy peaks corresponding to Ti^{4+} $2p_{3/2}$ and Ti^{4+} $2p_{1/2}$ electrons, and Ti^{0} $2p_{3/2}$ and Ti^{0} $2p_{1/2}$ electrons, respectively, as shown in Figure 4 (a). Furthermore, the W^{0} 4f spectrum was consisted of lower and higher binding energy peaks corresponding to W^{0} $4f_{7/2}$ and W^{0} $4f_{5/2}$ electrons. Similarly, the W^{ox} 4f spectrum was also composed of three doublets of the overlapped spectra of three oxidized species of tungsten (that is, doublets of W^{4+} $4f_{7/2}$ and W^{4+} $4f_{5/2;}$ W^{5+} $4f_{7/2}$ and W^{5+} $4f_{5/2;}$ and W^{6+} $4f_{7/2}$ and W^{6+} $4f_{5/2}$ electrons) as shown in Figure 4 (b).

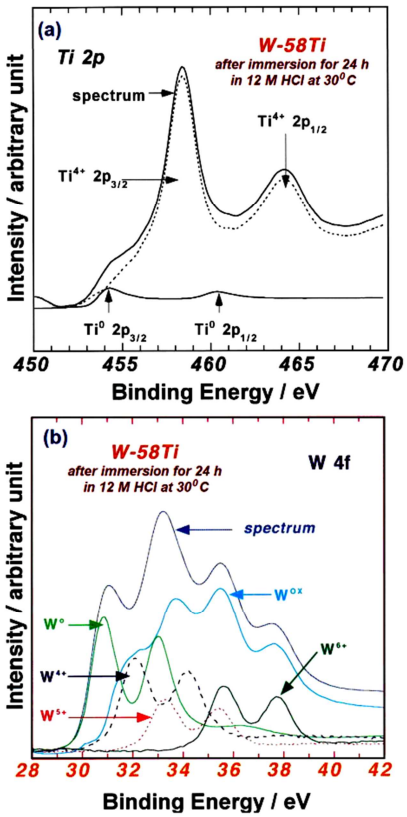

Figure 4. *Examples of the deconvolution of the (a) Ti 2p and (b) W 4f spectra measured for the W–58Ti alloy after immersion for 24 h in 12 M HCl solution open to air at 30 °C at the take-off angle of photoelectrons of 90°.*

The quantitative result of the in-depth compositional change of the surface films formed on the sputter-deposited W-xTi alloys using ARXPS analysis is shown in Figure 5. Figures 5 (a) and 5 (b) show the changes in apparent cationic fractions in the air-formed film after mechanical polishing as well as the spontaneously passivated films and the apparent atomic fractions in the underlying alloy surface of the W-22Ti and W-58Ti alloys after immersion for different periods of time in 12 M HCl solution open to air at 30°C, respectively, as a function of take-off angle of photoelectrons. Figure 5 clearly reveal that titanium is concentrated in the air-formed oxide films of the sputter-deposited W-xTi alloys as a result of preferential oxidation of titanium, while tungsten is significantly concentrated in the passive films of the alloys after immersion for 1-165 h in 12 M HCl.

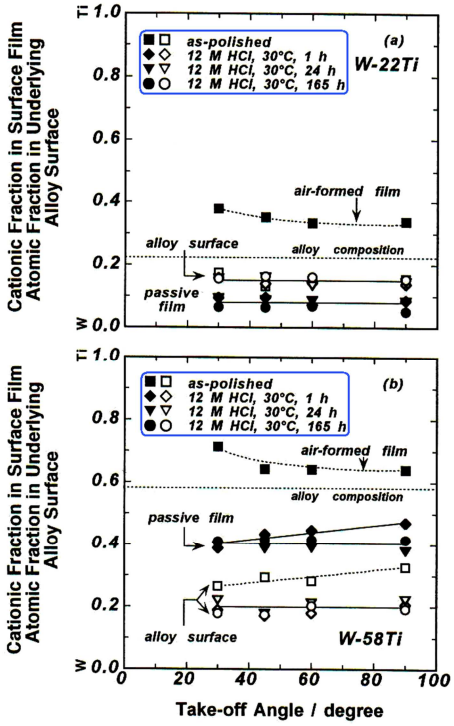

Figure 5. *Changes in the apparent (a) cationic fractions in the surface films and (b) atomic fractions in the underlying alloy surfaces for the sputter-deposited (a) W-22Ti and (b) W-58Ti alloys as a function of take-off angle of photoelectrons.*

There is no concentration gradient of tungsten and titanium ions in-depth of the passive surface film as well as the underlying alloy surface after immersion for different periods of time in such aggressive chloride containing solution of 12 M HCl, although a small concentration gradient of tungsten and titanium cations is observed in the air-formed film after exposing the mechanically polished W-22Ti and W-58Ti alloy specimens and in the passive film of the W-58Ti alloy after immersion for 1 h in 12 M HCl. Tungsten is slightly concentrated in the exterior part of the tungsten-rich passive film formed on the W-58Ti alloy after immersion for 1 h in 12 M HCl. However, after immersion for 24 hours or more the passive film becomes homogeneous without any concentration gradient in-depth.

On the other hand, there is a small concentration gradient of W^{ox} and Ti^{4+} cations with depth in the air-formed film as well as the underlying alloy surface. Accordingly, immersion in 12 M HCl for about 24 hours or more results in the formation of homogeneous passive films on the sputter-deposited W-xTi alloys. Consequently, the ARXPS measurement revealed that the formation of the spontaneous passive film composed of the homogeneous double oxyhydroxide of tungsten (W^{ox}) and titanium (Ti^{4+}) ions are responsible for extremely high corrosion resistance properties of the binary W-xTi alloy in aggressive chloride containing 12 M HCl solution. The changes in the ratios of W^{4+}, W^{5+} and W^{6+} ions in the surface films were determined quantitatively for a better understanding of the role of tungsten ions in the passive films formed on the W-xTi alloys.

Figure 6 shows the changes of the concentration ratios of W^{4+}, W^{5+} and W^{6+} ions to the total tungsten ions in the spontaneously passivated films formed on the W-22Ti and W-58Ti alloys after immersion for 24 hours in 12 M HCl solution open to air at 30°C, as a function of take-off angle of photoelectrons. After immersion for 24 h in 12 M HCl solution, the ratios of W^{6+} ion in the passive films formed on both the W-22Ti and W-58Ti alloys are significantly higher than those of W^{4+} and W^{5+} ions in the spontaneously passivated films. W^{6+} ion is decreased with increasing take-off angle of photoelectrons, while W^{4+} ion is increased with take-off angles. The ratio of W^{5+} ion is remained almost constant with take-off angle of photoelectrons.

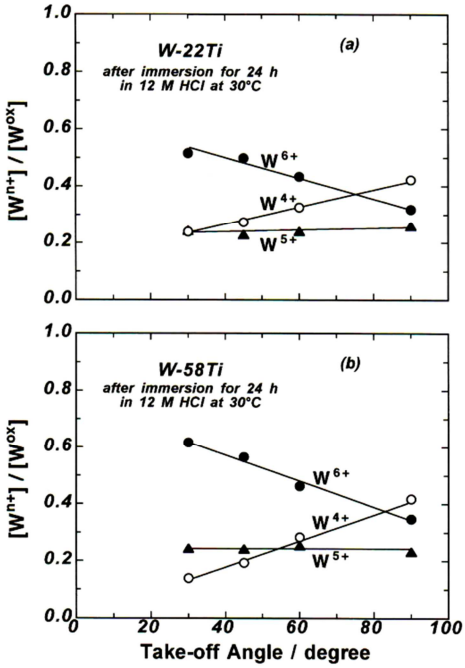

Figure 6. *The concentration ratios of W^{4+}, W^{5+} and W^{6+} ions to the total tungsten ions in the passive films formed on the (a) W-22Ti and (b) W-58Ti alloys after immersion for 24 h in 12 M HCl solution open to air at 30 °C as a function of take-off angle of photoelectrons.*

Accordingly, W^{4+} ion is particularly concentrated in the interior (at the take-off angle of 90°) of the spontaneously passivated films formed on the sputter-deposited W-xTi alloys, while the concentration of W^{6+} ion is higher in the exterior (at the take-off angles of 30 to 60°) of the spontaneously passivated films. It is

generally known that air exposure of the alloy specimen during the transfer from the electrolyte to the XPS analyzing chamber give rise to oxidation of W^{4+} to W^{6+} ion. Accordingly, the relative ratio of W^{6+} ion is higher in the exterior of the surface films and decreased with the depth of the passive films.

In general, one of the characteristics of the passive film is the concentration of oxygen species in the films formed on the corrosion-resistant alloys. Figure 7 shows the deconvolution of the O 1s spectra measure for the sputter-deposited W-58Ti alloy at different take-off angle of photoelectrons (that is, at 30°, 60° and 90° TOA) after immersion for 24 h in 12 M HCl solution open to air at 30°C. The spontaneously passivated films of W-58Ti alloy consists of oxyhydroxide in which O^{2-} ion is a major oxygen species, although the peaks correspond to OH^- ion and bound H_2O at low take-off angle of photoelectrons (that is, at 30° of take-off angle) is remarkably higher than that at the high take-off angles (that is, at 60° and 90° take-off angles).

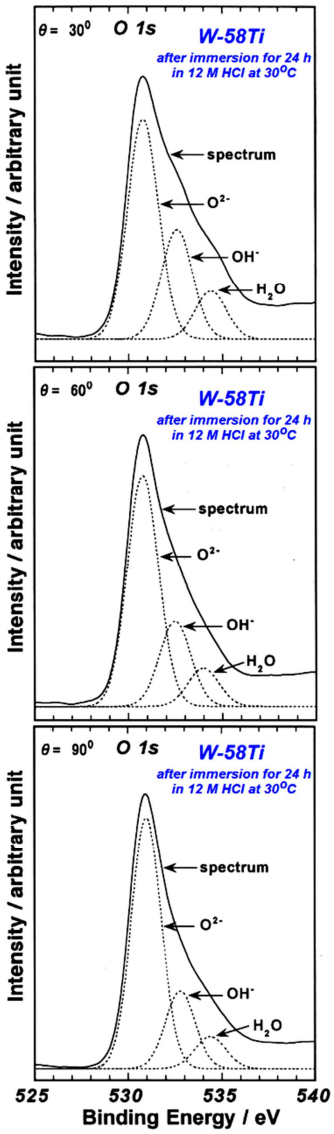

Figure 7. *An example of the deconvolution of O 1s spectra measured for the sputter-deposited W-58Ti alloy after immersion for 24 h in 12 M HCl solution open to air at 30℃ at different take-off angle of photoelectrons.*

Figure 8 shows the changes in the ratios of $[O^{2-}]$/[cations] and [OH]/[cations] in the spontaneously passivated films formed on the sputter-deposited W-22Ti and W-58Ti alloys after immersion for 24 h in 12 M HCl solution open to air at 30°C, as a function of take-off angle of photoelectrons. The ratio of $[O^{2-}]$/[cations] is slightly increased with the take-off angles and the ratio of [OH]/[cations] is significantly decreased with take-off angles in the films formed on the W-xTi alloys. Consequently, the interior part of the passive films of the sputter-deposited W-xTi alloys is rather dry and well developed by M–O–M bridging, while the exterior part of the passive films formed on the alloys is slightly wet with OH^- ion and H_2O.

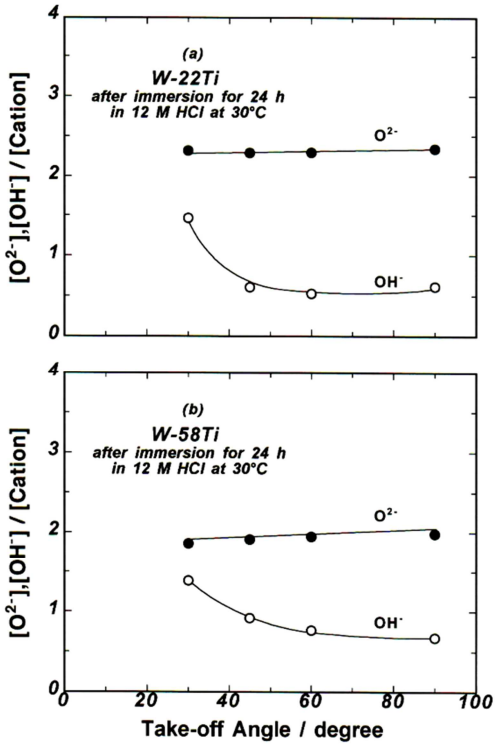

Figure 8. *Changes in the ratios of $[O^{2-}]$/[cations] and $[OH^-]$/[cations] in the surface films formed on the sputter-deposited amorphous W-22Ti and W-58Ti alloys after immersion for 24 h in 12 M HCl solution open to air at 30℃ as a function of take-off angle of photoelectrons.*

4. Conclusions

The mechanism of the synergistic effect of tungsten and titanium metals enhancing the higher corrosion resistance of the sputter-deposited W-xTi alloys than those of alloy-constituting elements has been studied by corrosion tests and angle resolved XPS measurements in 12 M HCl solution open to air at 30°C. The following conclusions are drawn:

1. The sputter-deposited W-xTi alloys were passivated spontaneously and hence they showed higher corrosion resistance than those of alloy-constituting elements.
2. The angle-resolved XPS measurement revealed that all cations of the binary W-xTi alloys are distributed homogeneously in the spontaneously passivated films formed on the alloys. The higher corrosion resistance of

the alloys than those of the alloy-constituting elements is mostly due to the formation of the homogeneous passive films composed of W^{4+} and Ti^{4+} ions without any concentration gradient in-depth.

3. The W^{4+} ion is particularly concentrated in the interior of the spontaneously passivated films formed on both the W-22Ti and W-58Ti alloys, while the concentration of W^{6+} ion is higher in the exterior of the passive films.
4. The interior part of the passive films of the W-xTi alloys is rather dry and well developed by M–O–M bridging, while the exterior part of the passive films of the alloys is slightly wet with OH^- ion and bound H_2O molecule.

Acknowledgements

The author is very thankful to Professors Emeritus; Dr. Koji Hashimoto and Dr. K. Asami of Tohoku University, Sendai, Japan for their kind permission to use the XPS machine, and would like to acknowledge to Profs; Dr. Hiroki Habazaki of Hokkaido University and Dr. Eiji Akiyama of IMR, Tohoku University, Japan for their fruitful discussion.

References

[1] L. A. Harris, Angular Dependences in Electron-excited Auger Emission, *Surf. Sci.,* 1969, 15 (1), 77-93. https://doi.org/10.1016/0039-6028(69)90066-1

[2] W. A. Fraser, J. V. Florio, W. N. Delgass, W. D. Robertson, Surface Sensitivity and Angular Dependence of X-ray Photoelectron Spectra, *Surf. Sci.,* 1973, 36 (2), 661-674. https://doi.org/10.1016/0039-6028(73)90410-X

[3] C. S. Fadley, Instrumentation for Surface Studies: XPS Angular Distributions, *J. Electron Spectros. Rel. Phenom.*, 1974, 5 (1), 725-754. https://doi.org/10.1016/0368-2048(74)85048-6

[4] C. S. Fadley, X-ray Photoelectron Spectroscopy: Progress and Perspectives, *J. Electron Spectros. Rel. Phenom.*, 2010, 178-179, 2-32. https://doi.org/10.1016/j.elspec.2010.01.006

[5] R. J. Baird, C. S. Fadley, X-ray Photoelectron Angular Distributions with Dispersion-compensating X-ray and Electron Optics, *J. Electron Spectros. Rel. Phenom.*, 1974, 11 (1), 39-65. https://doi.org/10.1016/0368-2048(77)85047-0

[6] M. Pijolat, G. Hollinger, New Depth-profiling Method by Angular-dependent X-ray Photoelectron Spectroscopy, *Surf. Sci.* 1981, 105 (1), 114-128. https://doi.org/10.1016/0039-6028(81)90151-5

[7] S. Tougaard, A. Ignatiev, Concentration Depth Profiles by XPS; A New Approach, *Surf. Sci.,* 1983, 129 (2-3), 355-365.. https://doi.org/10.1016/0039-6028(83)90186-3

[8] K. Siegbhahn, C. Nordling, A. Fahlman, R. Nordberg, K. Hamrin, J. Hedman, G. Johnssaon, T. Bergmark, S. E. Karlsson, I. Lindgren, B. Lindberg, *ESCA–Atomic, Molecular and Solid State Studied by Means of Electron Spectroscopy*, Almquist and Wiksells, Uppsal, Sweden, 1967.

[9] I. N. Demchenko, Y. Melikhov, Y. Syryanyy, I. Zaytseva, P. Konstantynoy, M. Chernyshova, Effect of Argon Sputtering on XPS Depth-profiling Results of Si/Nb/Si, *J. Electron Spectros. Rel. Phenom.*, 2018, 224, 17-22. https://doi.org/10.1016/j.elspec.2017.09.009

[10] S. R. Bare, A. Knop-Gericke, D. Teschner, M. Hävacker, R. Blume, T. Rocha, R. Schlögl, A. S. Y. Chan, N. Blackwell, M. E. Charochak, R. Veen, H. H. Brongersma, Surface Analysis of Zeolites: An XPS, Variable Kinetic Energy XPS, and Low Energy Ion Scattering Study, *Surf. Sci.*, 2016, 648, 376-382. https://doi.org/10.1016/j.susc.2015.10.048

[11] S. Tougaard, Energy loss in XPS: Fundamental Processes and Applications for Quantification, Non-destructive Depth Profiling and 3D Imaging, *J. Electron Spectros. Rel. Phenom.*, 2010, 178-179, 128-153. https://doi.org/10.1016/j.elspec.2009.08.005

[12] E. Akiyama, A. Kawashima, K. Asami, K. Hashimoto, A study of the Structure of a Passive Film Using Angle-resolved X-ray Photoelectron Spectroscopy, *Corros. Sci*., 1996, 38 (7), 1127-1140. https://doi.org/10.1016/0010-938X(96)81813-0

[13] P. Y. Park, E. Akiyama, A. Kawashima, K. Asami, K. Hashimoto, The Corrosion Behavior of Sputter-deposited Mo-Ti Alloys in Concentrated Hydrochloric Acid, *Corros. Sci.*, 1995, 38 (10), 1649-1667. https://doi.org/10.1016/S0010-938X(96)00041-8

[14] X. Y. Li, E. Akiyama, A. Kawashima, K. Asami, K. Hashimoto, Spontaneously Passivated Films on Sputter-deposited Cr-Ti Alloys in 6 M HCl Solution, *Corros. Sci.,* 1997, 39 (5), 935-948. https://doi.org/10.1016/S0010-938X(97)81159-6

[15] J. Bhattarai, E. Akiyama, H. Habazaki, A. Kawashima, K. Asami, K. Hashimoto, Electrochemical and XPS Studies of the Corrosion Behavior of Sputter-deposited Amorphous W-Zr Alloys in 6 and 12 M HCl Solutions, *Corros. Sci.,* 1997, 39 (2), 355-375. https://doi.org/10.1016/S0010-938X(97)83351-3

[16] J. Bhattarai, E. Akiyama, H. Habazaki, A. Kawashima, K. Asami, K. Hashimoto, Electrochemical and XPS Studies of the Corrosion Behavior of Sputter-deposited W-Nb Alloys in Concentrated Hydrochloric Acid Solutions, *Corros. Sci.,* 1998, 40 (1), 19-42. https://doi.org/10.1016/S0010-938X(97)00108-X

[17] J. Bhattarai, E. Akiyama, H. Habazaki, A. Kawashima, K. Asami, K. Hashimoto, Electrochemical and XPS Studies on the Passivation Behavior of Sputter-deposited W-Cr Alloys in 12 M HCl Solution, *Corros. Sci.,* 1998, 40 (2-3), 155-175. https://doi.org/10.1016/S0010-938X(97)00106-6

[18] J. Bhattarai, E. Akiyama, H. Habazaki, A. Kawashima, K. Asami, K. Hashimoto, The Passivation Behavior of Sputter-deposited W-Ta Alloys in 12 M HCl, *Corros. Sci.,* 1998, 40 (4-5), 757-779. https://doi.org/10.1016/S0010-938X(97)00177-7

[19] P. Marcus, Surface Science Approach of Corrosion Phenomena, *Electrochimica Acta*, 1998, 43 (1-2), 109-118. https://doi.org/10.1016/S0013-4686(97)00239-9

[20] J. Bhattarai, Angle Resolver X-Ray Photoelectron Spectroscopic Analysis of the Passive Film of the Corrosion-Resistant W-32Zr Alloy in 12 M HCl Solution, *Bangladesh J. Sci. Ind. Res.*, 2014, 49 (2), 103-110. http://dx.doi.org/10.3329/bjsir.v49i2.22004

[21] J. Bhattarai, X-ray Photoelectron Spectroscopic Analyses on the Corrosion-Resistant W-Cr-Ni Alloys in 12 M HCl, *Trans. Mater. Res. Soc. Jpn.,* 2010, 35 (1), 1-6. https://doi.org/10.14723/tmrsj.35.1

[22] J. Bhattarai, A Non–destructive Compositional Analysis of Thin Surface Films Formed on W-xTa Alloys by Angle Resolved X-ray Photoelectron Spectroscopy, *Bibechana*, 2012, 8, 8-16. https://doi.org/10.3126/bibechana.v8i0.4784

[23] K. Hashimoto, Chemical Properties of Rapidly Solidified Alloys, in H. H. Liebermann (ed.) *Rapidly Solidified Alloys; Processes, Structures, Properties, Applications*, Marcel Dekker Inc., New York, 1993, pp. 591.

[24] S. Baral, J. Bhattarai, The Effect of Tantalum Addition on the Corrosion Behavior of W-xTa Alloys in 1 M NaOH Solution, *Bibechana*, 2014, 10, 1-8. https://dx.doi.org/10.3126/bibechana.v10i0.8363

[25] P. L. Kharel, S. P. Sah, J. Bhattarai, Roles of Alloying Elements on the Passivity of W-xCr-yNi Alloys in Aggressive Environments, *Nepal J. Sci. Technol.*, 2013, 14 (2), 73-80. https://dx.doi.org/10.3126/njst.v14i2.10418

[26] J. Bhattarai, X-ray Photoelectron Spectroscopic Study on the Anodic Passivity of Sputter-deposited W-Nb Alloys in 12 M HCl Solution, *J. Sci. Res.*, 2011, 3 (3), 467-480. https://dx.doi.org/10.3329/jsr.v3i3.7207

[27] B. R. Aryal, J. Bhattarai, Effects of Tungsten, Chromium and Zirconium on the Corrosion Behavior of Ternary Amorphous W-Cr-Zr Alloys in 1 M NaOH Solution, *Sci. World*, 2011, 9, 39-43. https://dx.doi.org/10.3126/sw.v9i9.5516

[28] J. Bhattarai, The Corrosion Behavior of Sputter-deposited Ternary W-Zr-(15-18)Cr Alloys in 12 M HCl, *Afr. J. Pure Appl. Chem.*, 2011, 5 (8), 212-218.

[29] J. Bhattarai, Role of Alloying Elements on the Corrosion Behavior of Sputter-deposited Amorphous W-Cr-Zr Alloys in 0.5 M NaCl Solution, *Sci. World*, 2011, 9, 34-38 (2011). http://dx.doi.org/10.3126/sw.v9i9.5515

[30] P. Shrestha, J. Bhattarai, The Passivation Behavior of Sputter-deposited W-Zr Alloys in NaCl and NaOH Solutions, *J. Nepal Chem. Soc.*, 2010, 25, 37-45. https://dx.doi.org/10.3126/jncs.v25i0.3283

[31] R. R. Kumal, J. Bhattarai, Roles of Alloying Elements on the Corrosion Behavior of Amorphous W-Zr-(15-33)Cr Alloys in 1 M NaOH Solution, *J. Nepal Chem. Soc.*, 2010, 25, 93-100. https://dx.doi.org/10.3126/jncs.v25i0.3312

[32] J. Bhattarai, The Corrosion Behavior of Sputter-deposited Ternary Zr-(12-18)Cr-W Alloys in 12 M HCl Solution, *J. Nepal Chem. Soc*., 2010, 26, 13-21. https://doi.org/10.3126/jncs.v26i0.3625

[33] M. Basnet, J. Bhattarai, The Corrosion Behavior of Sputter-Deposited Nanocrystalline W-Cr Alloys in NaCl and NaOH Solution, *J. Nepal Chem. Soc*., 2010, 25, 53-61. https://doi.org/10.3126/jncs.v25i0.3300

[34] B. R. Aryal, J. Bhattarai, Effects of Alloying Elements on the Corrosion Behavior of Sputter-deposited Zr-(12-21)Cr-W Alloys in 0.5 M NaCl Solution, *J. Nepal Chem. Soc.*, 2010, 25, 75-82. https://dx.doi.org/10.3126/jncs.v25i0.3305

[35] A. Khadka, J. Bhattarai, Corrosion and Electrochemical Properties of Nanocrystalline W-Mo Alloys in NaOH Solution, *Nepal J. Sci. Technol.*, 2010, 11, 147-151. https://doi.org/10.3126/njst.v11i0.4137

[36] J. Bhattarai, The Effects of Chromium and Nickel on the Passivation Behavior of Sputter-deposited W-Cr-Ni Alloys in 12 M HCl Solution, *Sci. World*, 2009, 7 (7), 24-28. https://doi.org/10.3126/sw.v7i7.3819

[37] S. P. Sah, J. Bhattarai, The Electrochemical and Surface Studies of the Corrosion Behavior of Sputter-deposited W-Ni Alloys in 0.5 M NaCl Solution, *J. Nepal Chem. Soc.*, 2009, 23, 45-53. https://dx.doi.org/10.3126/jncs.v23i0.2096

[38] J. Bhattarai, P. L. Kharel, Effects of Chromium and Tungsten on the Corrosion Behavior of Sputter-deposited W-Cr-Ni Alloys in 0.5 M NaCl Solution, *J. Inst. Sci. Technol.*, 2009, 16, 141-151.

[39] P. L. Kharel, J. Bhattarai, The Corrosion Behavior of Sputter-deposited W-Cr-(4-15)Ni Alloys in NaOH Solution, *J. Nepal Chem. Soc.*, 2009, 24, 3-11. https://dx.doi.org/10.3126/jncs.v24i0.2380

[40] H. Jha, J. Bhattarai, Corrosion Behavior of Sputter-deposited W-Nb Alloys in NaCl and NaOH Solutions, *J. Alloys Compd.*, 2008, 456, 474-478. https://dx.doi.org/10.1016/j.jallcom.2007.02.100

[41] J. Bhattarai, Structure and Corrosion Behavior of Sputter-deposited W-Mo Alloys, *J. Nepal Chem. Soc.*, 2006, 21, 19-25. https://doi.org/10.3126/jncs.v21i0.217

[42] J. Bhattarai, The Role of Tungsten in the Passivation Behavior of Sputter-deposited Cr-9W Alloy in 12 M HCl, *J. Inst. Sci. Technol.*, 2002, 12, 125-138.

[43] J. Bhattarai, Electrochemical and XPS Studies on the Corrosion Behavior of Sputter-deposited Amorphous W-Ni Alloys in 12 M HCl, *J. Nepal Chem. Soc.*, 2001, 20, 24-40.

[44] J. Bhattarai, E. Akiyama, H. Habazaki, A. Kawashima, K. Asami, K. Hashimoto, The Influence of Concentration of Hydrochloric Acid Solutions on the Passivation Behavior of Sputter-Deposited Tungsten Rich W–Nb Alloys, *Corros. Sci.,* 1998, 40 (11), 1897-1914. https://doi.org/10.1016/S0010-938X(98)00088-2

[45] J. Bhattarai, K. Hashimoto, X-Ray Photoelectron Spectroscopy Study in the Anodic Passivity of Sputter-Deposited Nanocrystalline W-Cr Alloys in 12 M HCl. *Tribhuvan Univ. J.*, 1998, 21 (2), 1-16. https://doi.org/10.3126/tuj.v21i2.4568

[46] K. Asami, S. C. Chen, H. Habazaki, A. Kawashima, K. Hashimoto, A Photo-electrochemical and ESCA Study of Passivity of Amorphous Nickel-valve Metal Alloys, *Corros. Sci.*, 1990, 31, 727-732. https://doi.org/10.1016/0010-938X(90)90188-B

[47] K. Asami, S. C. Chen, H. Habazaki, K. Hashimoto, The Surface Characterization of Titanium and Titanium-nickel Alloys in Sulfuric Acid, *Corros. Sci.,* 1993, 35, 43-49. https://doi.org/10.1016/0010-938X(93)90131-Y

[48] J. H. Kim, E. Akiyama, H. Yoshioka, H. Habazaki, A. Kawashima, K. Asami and K. Hashimoto, The Corrosion Behavior of Sputter-deposited Amorphous Titanium-chromium Alloys in 1 M and 6 M HCl Solutions, *Corros. Sci.*, 1993, 34 (6), 975-987. https://doi.org/10.1016/0010-938X(93)90074-Q

[49] K. Hashimoto, K. Asami, A. Kawashima, H. Habazaki, E. Akiyama, The Role of Corrosion-resistant Alloying Elements in Passivity, *Corros. Sci.,* 2007, 49 (1), 42-52. https://doi.org/10.1016/j.corsci.2006.05.003

[50] J. Bhattarai, The Corrosion Behavior of Sputter-deposited W-Ti Alloys in 0.5 M NaCl Solution, *Nepal J. Sci. Technol.,* 2009, 10, 109-114. https://doi.org/10.3126/njst.v10i0.2899

[51] A. Sharmah, H. Jha, J. Bhattarai, The Passivation Behavior of Sputter-Deposited W-Ti Alloys in 1 M NaOH Solution, *J. Nepal Chem. Soc.,* 2007, 22, 17-25. https://doi.org/10.3126/jncs.v22i0.518

[52] J. Bhattarai, K. Hashimoto, The Anodic Passivity of Sputter-deposited W-Ti Alloys in Hydrochloric Solutions, *Nepal J. Sci. Technol*., 2002, 4 (1), 37-43. http://www.nast.org.np/njst/index.php/njst/article/view/84/69

[53] J. Bhattarai, E. Akiyama, A. Kawashima, K. Asami, K. Hashimoto, The Corrosion Behavior of Sputter-deposited Amorphous W-Ti Alloys in 6 M HCl Solution, *Corros. Sci.,* 37 (12), 1995, 2071-2086. https://doi.org/10.1016/0010-938X(95)00120-9

[54] J. Bhattarai, The Confocal Scanning Laser Microscopic Study of the Pitting Corrosion on Sputter-deposited W-Ti Alloys in 1 M NaOH Solution, *Tribhuvan Univ. J.*, 2009, 26 (1), 17-26. https://doi.org/10.3126/tuj.v26i1.2611

[55] A. A. El-Moneim, B. P. Zhang, E. Akiyama, H. Habazaki, A. Kawashima, K. Asami, K. Hashimoto, The Corrosion Behavior of Sputter-deposited Amorphous Mn-Ti Alloys in 0.5 M NaCl Solution, *Corros. Sci.,* 1997, 39 (2), 305-320. https://doi.org/10.1016/S0010-938X(96)00128-X

[56] Y.-D. Im, Y.-K. Lee, Effects of Mo Concentration on Re-crystallization Texture, Deformation Mechanism and Mechanical Properties of Ti-Mo Binary Alloys, *J. Alloys Compd.*, 2020, 821, 153508. https://doi.org/10.1016/j.jallcom.2019.153508

[57] N. Kang, Y. Li, X. Lin, E. Feng, W. Huang, Microstructure and Tensile Properties of Ti-Mo Alloys Manufactured via Using Laser Powder Bed Fusion, *J. Alloys Compd.*, 2019, 771, 877-884. https://doi.org/10.1016/j.jallcom.2018.09.008

[58] M. Callisti, F. D. Tichelaar, T. Polcar, In situ TEM Observations on the Structural Evolution of a Nanocrystalline W-Ti Alloy at Elevated Temperatures, *J. Alloys Compd.*, 2018, 749, 1000-1008. https://doi.org/10.1016/j.jallcom.2018.03.335

[59] C.-L. Chen, Y. Zeng, Influence of Ti Content on Synthesis and Characteristics of W-Ti ODS Alloy, *J. Nucl. Mater.*, 2016, 469, 1-8. https://doi.org/10.1016/j.jnucmat.2015.11.018

[60] M. Buzatu, V. Geantă, R. Ștefănoiu, M. Buțu, M.-I. Petrescu, M. Buzatu, I. Antoniac, G. Iacob, F. Niculescu, S.-I. Ghica, H. Moldovan, Investigations into Ti-15Mo-W Alloys Developed for Medical Applications, *Materials*, 2019, 12 (1), 147. https://doi.org/10.3390/ma12010147

[61] M. Buzatu, S. I. Ghica, M. I. Petrescu, V. Geantă, R. Stefănoiu, G. Iacob, M. Butu, E. Vasile, Obtaining and Characterization of the Ti15Mo5W Alloy for Biomedical Applications. *Mater. Plast.*, 2017, 54 (3), 596-600. https://doi.org/10.37358/MP.17.3.4905

[62] B. D. Cullity, Elements of X-ray Diffraction, 2nd edition, Addison-Wesley Publ. Co. Inc., p. 101 (1977).

[63] B. N. Subedi, K. Amgain, S. Joshi, J. Bhattarai, Green Approach to Corrosion Inhibition Effect of *Vitex negundo* Leaf Extract on Aluminum and Copper Metals in Biodiesel and its Blend, *Int. J. Corros. Scale Inhib*., 2019, 8 (3), 744-759. https://doi.org/10.17675/2305-6894-2019-8-3-21

[64] M. Rana, S. Joshi, J. Bhattarai, Extract of Different Plants of Nepalese Origin as Green Corrosion Inhibitor for Mild Steel in 0.5 M NaCl Solution, *Asian J. Chem.*, 2017, 29 (5) 1130-1134. https://doi.org/10.14233/ajchem.2017.20449

[65] K. Asami, K. Hashimoto, The X-ray Photo-electron Spectra of Several Oxides of Iron and Chromium, *Corros. Sci.*, 1977, 17 (7), 559-570. https://doi.org/10.1016/S0010-938X(77)80002-4

[66] K. Asami, A Precisely Consistent Energy Calibration Method for X-ray Photoelectron Spectroscopy, *J. Electron Spectros. Rel. Phenom.*, 1976, 9 (5), 469-478. https://doi.org/10.1016/0368-2048(76)80065-5

[67] A. Kawashima, K. Asami, K. Hashimoto, An XPS Study of Anodic Behavior of Amorphous Nickel-phosphorus Alloys Containing Chromium, Molybdenum or Tungsten in 1 M HCl, *Corros. Sci.,* 1994, 24 (9), 807-823. https://doi.org/10.1016/0010-938X(84)90029-5